Chapter 22

Determination of the ATP Affinity of the Sarcoplasmic Reticulum Ca^{2+}-ATPase by Competitive Inhibition of [γ-^{32}P] TNP-8N_3-ATP Photolabeling

Johannes D. Clausen, David B. McIntosh, David G. Woolley, and Jens Peter Andersen

Abstract

The photoactivation of aryl azides is commonly employed as a means to covalently attach cross-linking and labeling reagents to proteins, facilitated by the high reactivity of the resultant aryl nitrenes with amino groups present in the protein side chains. We have developed a simple and reliable assay for the determination of the ATP binding affinity of native or recombinant sarcoplasmic reticulum Ca^{2+}-ATPase, taking advantage of the specific photolabeling of Lys^{492} in the Ca^{2+}-ATPase by [γ-^{32}P]2′,3′-O-(2,4,6-trinitrophenyl)-8-azido-adenosine 5′-triphosphate ([γ-^{32}P]TNP-8N_3-ATP) and the competitive inhibition by ATP of the photolabeling reaction. The method allows determination of the ATP affinity of Ca^{2+}-ATPase mutants expressed in mammalian cell culture in amounts too minute for conventional equilibrium binding studies. Here, we describe the synthesis and purification of the [γ-^{32}P]TNP-8N_3-ATP photolabel, as well as its application in ATP affinity measurements.

Key words ATP binding affinity, Photoaffinity labeling, [γ-^{32}P]TNP-8N_3-ATP synthesis, Sarcoplasmic reticulum Ca^{2+}-ATPase, Ca^{2+}-ATPase mutants, P-type ATPase family

1 Introduction

P-type ATPases bind ATP with high affinity, typically displaying dissociation constants in the 0.1–10 μM range for the interaction of the Mg^{2+}·ATP complex with the high-affinity nucleotide-binding site of the *E*1 state of the enzyme. When a relatively pure source of the ATPase protein is available, ATP binding studies can be carried out directly in equilibrium binding assays [1–5]. However, in circumstances where the ATPase only represents a minor fraction of the total protein in the sample, as is typically the case when the ATPase is obtained by heterologous expression in mammalian cell culture, it is generally not feasible to measure ATP binding directly. An indirect measure of the ATP affinity of recombinant ATPase

Maike Bublitz (ed.), *P-Type ATPases: Methods and Protocols*, Methods in Molecular Biology, vol. 1377,
DOI 10.1007/978-1-4939-3179-8_22,

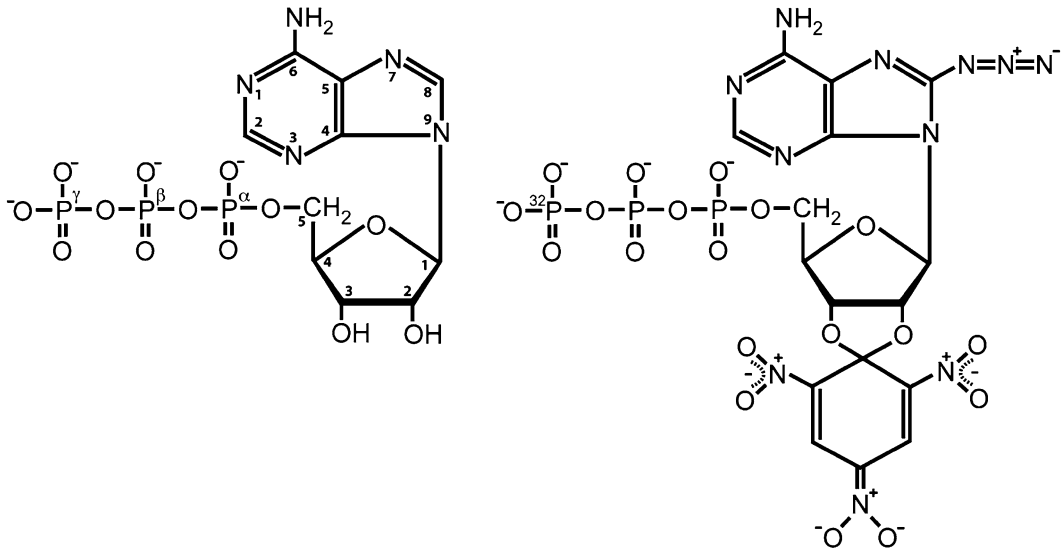

Fig. 1 Schematic structures of ATP (*left*) and [γ-^{32}P]TNP-8N_3-ATP (*right*). The [γ-^{32}P]TNP-8N_3-ATP photolabel is a derivative of ATP, formed by the addition of an azido group to the 8-position of the adenine and a TNP group to the 2′,3′-positions of the ribose, and by the exchange of the γ-phosphate with a ^{32}P-labeled phosphate

expressed in relatively low yield can often be obtained by studying the ATP dependence of a given functional characteristic, such as the phosphorylation by [γ-^{32}P]ATP (either the steady-state level or the transient kinetics) or the rate of overall ATP turnover [6–9]. Such measurements are, however, easily influenced by shifts in the protein conformational transitions towards or away from the ATP-reactive *E*1 state (often relevant for the study of mutant ATPases) and generally need to be interpreted in the light of a detailed investigation of other partial reaction steps in the ATPase cycle in order to permit trustworthy conclusions regarding the "true" ATP affinity.

We have developed an assay [10] that enables the direct determination of ATP affinity constants for the sarcoplasmic reticulum Ca^{2+}-ATPase, overcoming the technical difficulties associated with ATP binding measurement on the minute amounts of wild type or mutant Ca^{2+}-ATPase present in microsomes purified from transfected mammalian cell cultures. The assay makes use of the ATP-analogue [γ-^{32}P]TNP-8N_3-ATP, taking advantage of three unique features of this compound relative to ATP (Fig. 1): (a) a photoactivatable azido (N_3) group at the 8-position of the adenine, enabling the covalent coupling of the nucleotide to the ATPase [11–14], (b) a TNP moiety at the 2′,3′-positions of ribose, providing the nucleotide with an increased affinity and specificity for the ATPase relative to that of ATP [15, 16], and (c) a ^{32}P-labeled γ-phosphate, enabling radiometric detection of the labeled protein. Upon UV irradiation of the Ca^{2+}-ATPase in a reaction mix containing [γ-^{32}P]TNP-8N_3-ATP, this nucleotide becomes covalently attached via

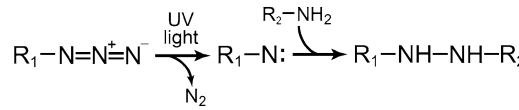

Fig. 2 Photolabeling of the Ca^{2+}-ATPase by TNP-$8N_3$-ATP. The azido group of TNP-$8N_3$-ATP is activated by ultraviolet light, leading to the formation of a short-lived but highly reactive nitrene group. The nitrene can initiate reactions with neighboring reactive groups, such as the amino group of the Lys^{492} side chain in the Ca^{2+}-ATPase, thereby forming a stable covalent bond between the nucleotide and the protein [11–13]. R_1 represents the TNP-ATP part of TNP-$8N_3$-ATP (*see* Fig. 1), and R_2 is the Lys^{492} side chain

the azido group to a specific lysine, Lys^{492}, in the nucleotide-binding domain of the ATPase [11, 17, 18] (Fig. 2). Addition of non-radioactive ATP competitively inhibits the photolabeling reaction, and titration of the ATP dependence of the inhibition of photolabeling provides a means to determine binding of ATP to the enzyme [10]. Our studies have shown that the dissociation constants obtained by this method are remarkably similar to those obtained by conventional equilibrium binding methods when direct comparisons are made under identical conditions. This approach furthermore has the advantage over traditional direct and indirect nucleotide binding assays that it is not limited to the analysis of ATP binding to one specific intermediate state in the Ca^{2+}-ATPase reaction cycle, as is generally the case for assays measuring the ATP dependence of a given functional characteristic, but can be carried out on any reaction state that can be stabilized in vitro, owing to the high affinity of the Ca^{2+}-ATPase for TNP-$8N_3$-ATP throughout the reaction cycle. Thus, the assay enables the determination of ATP dissociation constants, not only for the catalytic high-affinity binding mode in the *E*1 state of the reaction cycle [10], but also for the regulatory binding modes in the *E*2 and *E*2P states [16, 19]. Our [γ-^{32}P]TNP-$8N_3$-ATP photolabeling studies of Ca^{2+}-ATPase mutants [10, 16, 19–28] have identified residues crucial to ATP binding, later confirmed by X-ray crystal structures of the Ca^{2+}-ATPase with bound ATP-analogs [29–32]. Hence, the importance of the conserved phenylalanine of the N-domain, Phe^{487}, in ATP binding by the Ca^{2+}-ATPase (Fig. 3 and Table 1) was first demonstrated in [γ-^{32}P]TNP-$8N_3$-ATP photolabeling studies [10].

The ability to undergo photolabeling from TNP-$8N_3$-ATP has, thus far, only been demonstrated for one member of the P-type ATPase family, namely the rabbit SERCA1a isoform of the sarcoplasmic reticulum Ca^{2+}-ATPase. It is well known, however, that trinitrophenylated nucleotides bind with high affinity to other P-type ATPases as well, including the Na^+,K^+-ATPase [33, 34] and the H^+,K^+-ATPase [35, 36]. The lysine that is labeled by TNP-$8N_3$-ATP in the Ca^{2+}-ATPase, Lys^{492} (Fig. 3), is highly conserved

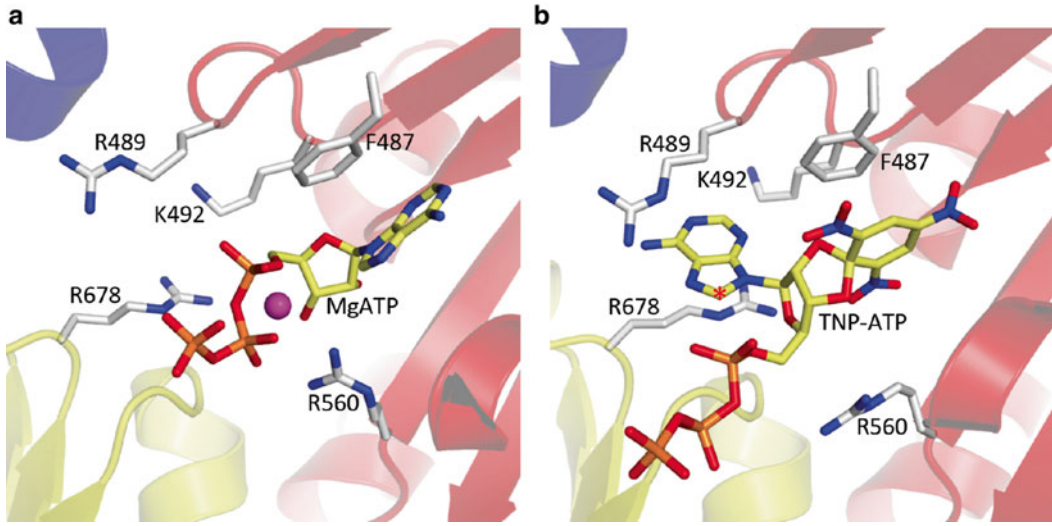

Fig. 3 Structural organization of the nucleotide binding site in the Ca^{2+}-ATPase. The structures shown are (**a**) *E2*·thapsigargin·Mg^{2+}·ATP (PDB 3AR4) and (**b**) *E2*·thapsigargin·TNP-ATP (PDB 3AR7) [47]. The N domain is shown in *red cartoon*, the A domain in *blue cartoon*, the P domain in *yellow cartoon*, the nucleotides and relevant side chains in *stick model* (*yellow* and *grey carbons*, respectively), and a Mg^{2+}-ion as a *purple sphere*. The TNP-moiety of TNP-ATP occupies the binding pocket that normally coordinates the adenine moiety of ATP. TNP-ATP is in the anti-conformation around the glycosidic bond, whereas TNP-$8N_3$-ATP would be expected to be mainly in the syn-conformation, owing to electrostatic repulsion between the azido-group and the phosphate-moiety [48]. The Lys^{492} side chain is positioned such that it would be in close proximity to the 8-position (marked by a *red asterisk* in panel **b**) of the adenine if the nucleotide were in the syn-conformation, in accordance with the fact that Lys^{492} is the residue that is photolabeled by TNP-$8N_3$-ATP [17]

throughout the P-type ATPase family (Table 1), being absent only in ATPases of the P_{1A} type (bacterial K^+-pumps; the lysine being replaced by an arginine), the P_{1B} type (heavy-metal pumps), and the P_5 type (ATPases with unassigned specificity) [37, 38]. With respect to the remaining seven P-type ATPase subfamilies, the lysine is conserved in 207 of 210 sequences analyzed [37]. It is therefore likely, that the ATP binding assay described here can be applied also with other P-type ATPases. Indeed, the assay is not only limited to transporters of the P-type ATPase family. Hence, both p-glycoprotein and Yor1p, two members of the family of ABC (ATP-binding cassette) transporters, are likewise able to become specifically photolabeled at their nucleotide-binding sites by TNP-$8N_3$-ATP, facilitating the determination of ATP-binding affinities in the same type of competition assays described here [39, 40].

The photolabeling assay itself is relatively easy and straightforward to carry out. The [γ-^{32}P]TNP-$8N_3$-ATP photolabel, however, is not commercially available, and needs to be prepared in the laboratory. In the following, we present a detailed protocol for the synthesis and purification of high specific activity [γ-^{32}P]TNP-$8N_3$-ATP, using commercially available $8N_3$-ATP as starting material. We subsequently describe the procedure for the application of

Table 1
Conservation in the family of P-type ATPases of the ^{487}Phe-Ser-Arg-Asp-Arg-Lys^{492} nucleotide-binding motif, containing the lysine residue that is specifically labeled by TNP-8N_3-ATP in the Ca^{2+}-ATPase. The analysis is based on the protein sequences listed in the P-type ATPase database available on the World Wide Web [37, 38]

Subfamily	Substrate specificity	# Sequences[a]	Sequence conservation[b]
P_{1A}	Unassigned	6	FtAxtR
P_{1B}	Cu^+, Ag^+, Cu^{2+}, Cd^{2+}, Zn^{2+}, Pb^{2+}, Co^{2+}	71	-[c]
P_{2A}	Ca^{2+}, Mn^{2+} (incl. SERCA pumps)	57	FsrxrK
P_{2B}	Ca^{2+} (incl. PMCA pumps)	26	FnSxrK
P_{2C}	Na^+/K^+, H^+/K^+	43	FNStnK
P_{2D}	Unassigned	8	FDSxxK
P_{3A}	H^+	39	FxPvdK
P_{3B}	Mg^{2+}	3	FLDPPK
P_4	Phospholipids	34	FxsxrK
P_5	Unassigned	16	Fxsxlx

[a]The total number of protein sequences included in the analysis is listed for each subfamily.
[b]Amino acid sequence conservation within each subfamily of P-type ATPases. *Uppercase letter*, amino acid (single-letter code) conserved in > 95 % of the sequences in the database; *lower case letter*, amino acid conserved in 60–95 % of the sequences in the database; *x*, < 60 % amino acid conservation.
[c]The FxxxxK nucleotide-binding motif generally found in the P-type ATPase family is not present in ATPases of the P_{1B} subfamily, which instead rely on a variant motif, where a histidine residue provides the π-stacking interaction with the adenine moiety of ATP [46] rather than a phenylalanine, as found at the corresponding position in the nine other P-type ATPase subfamilies (e.g., Phe^{487} in the Ca^{2+}-ATPase; *see* Fig. 3).

[γ-^{32}P]TNP-8N_3-ATP in competition experiments, exemplified by the determination of the ATP affinity of COS-1-expressed wild type and mutant Ca^{2+}-ATPase stabilized in the *E*2·P phosphate transition state.

2 Materials

All solutions and dilutions are aqueous, prepared using deionized water filter-purified to a sensitivity of 18 MΩ. Unless stated otherwise, buffers and solutions are stored at room temperature. When indicated, solutions are filter sterilized using 0.22 μm pore size syringe filters.

2.1 Preparation of [γ-^{32}P]TNP-8N_3-ATP

1. 10 mM 8N_3-ATP pH 7.6 (BIOLOG Life Science Institute, Bremen, Germany; *see* **Note 1**). Store at −20 °C.
2. ^{32}P-exchange buffer (10×): 1 M Tris/HCl, pH 8.0, 60 mM $MgCl_2$. Filter sterilize and store in small aliquots at −20 °C.

3. 100 mM NaOH. Filter sterilize and store in small aliquots at −20 °C.
4. 500 mM L-cysteine. Store in small aliquots at −20 °C.
5. 100 mM d-(-)-3-phosphoglyceric acid. Store in small aliquots at −20 °C.
6. Glyceraldehyde 3-phosphate dehydrogenase. Supplied as a lyophilized powder. Dissolve in water to give a protein concentration of 27 mg/mL. Store at −20 °C.
7. 3-Phosphoglyceric phosphokinase. Supplied as an ammonium sulfate suspension, typically with a protein concentration of 3–4 mg/mL. Store at 4 °C. After first use, carefully seal the lid to prevent water evaporation.
8. Phosphorus-32 orthophosphoric acid in water, 10 mCi/mL. *See* **Note 2**.
9. Dilutions of HCl at concentrations of 1 mM, 10 mM, 30 mM, and 1 M.
10. 0.8 M Na_2CO_3/$NaHCO_3$, pH 9.5: Dissolve 0.91 g Na_2CO_3 and 0.63 g $NaHCO_3$ in 10 mL water by stirring and heating to ~37 °C. Store in aliquots of 0.5 mL at −20 °C.
11. 1 M 2,4,6-trinitrobenzenesulfonic acid (TNBS; sold by Sigma-Aldrich under the name *Picrylsulfonic acid solution, 1 M in* H_2O). Store at −20 °C.
12. 5,5′-Dithiobis(2-nitrobenzoic acid) (DTNB).
13. 0.2, 0.5, and 1 M ammonium formate, pH 8.2: Prepare the 1 M solution by dissolving 3.15 g ammonium formate in 45 mL water and adjusting the pH to 8.2 with ammonia. Add water to a final volume of 50 mL. Prepare the 0.2 and 0.5 mM solutions by diluting the 1 M solution in water (10 mL water + 10 mL 1 M ammonium formate, and 10 mL water + 2.5 mL 1 M ammonium formate, respectively). Prepare fresh prior to use.
14. 500 mM KH_2PO_4/K_2HPO_4, pH 6.7: Prepare 500 mM solutions of both KH_2PO_4 and K_2HPO_4, and then adjust the pH of the 500 mM KH_2PO_4 solution to 6.7 with the 500 mM K_2HPO_4 solution. Filter sterilize and store at 4 °C.
15. 10 mM KH_2PO_4/K_2HPO_4, pH 7.0: 0.4 mL 500 mM KH_2PO_4/K_2HPO_4, pH 6.7 + 19.6 mL water. Filter sterilize and store at 4 °C.
16. 60 % (v/v) acetonitrile: 30 mL 100 % acetonitrile + 20 mL water. Filter sterilize.
17. Whatman® DE52 pre-swollen microgranular anion exchange cellulose (GE Healthcare Life Sciences, Pittsburgh, PA, USA).
18. Two 10 cm × 0.5 cm (inner diameter) Glass Econo-Column® columns for gravity flow chromatography (Bio-Rad, Hercules, CA, USA) with outlet tubing of 1 and 2 mL dead-volume, respectively.

19. Sep-Pak® Plus C18 Cartridges for solid phase extraction (Waters, Milford, MA, USA).
20. Methanol.
21. 1, 2, 5, 10, and 20 mL plastic syringes.
22. pH indicator strips (not essential).
23. TLC PEI Cellulose F thin layer chromatography (TLC) sheets, 20 × 20 cm (Merck-Millipore, Billerica, MA, USA).
24. Mobile solvent for TLC: 1 M LiCl.
25. Hair dryer (for drying the TLC sheets).
26. Liquid nitrogen.
27. Nitrogen gas cylinder.
28. Freeze-drying equipment: We use a homemade freeze-drying setup consisting of a vacuum pump, capable of creating a vacuum of < 0.1 mbar (critical!), connected via a cold trap to a temperature- and vacuum-resistant Pyrex Quickfit FR50/3S 50 mL round-bottomed flask (Scilabware, Stoke-on-Trent, UK).
29. Incubator oven at 25 °C; not necessary if the room temperature is already around 25 °C (± 3–4°).
30. Temperature-regulated water bath.
31. A Geiger-Müller counter.
32. Thick (~1 cm) acrylic glass protection as well as several thick-walled lead containers for the protection against concentrated radioactivity (*see* **Note 3**).
33. Radiometric detection equipment: We use a PerkinElmer Cyclone Plus Phosphor Imager with MultiSensitive Phosphor Screens. The Optiquant software package (PerkinElmer) is used for quantification of the radioactive gel bands and TLC spots.
34. Spectrophotometric equipment, ideally with the option of creating a full absorbance spectrum between 200 and 600 nm.

2.2 [γ-^{32}P]TNP-8N_3-ATP Photolabeling of the Ca^{2+}- ATPase

1. 25 % tetramethyl ammonium hydroxide (TMAH) solution (*see* **Note 4**).
2. Ca^{2+}-ATPase storage buffer: 5 mM 4-(2-hydroxyethyl)-piperazine-1-ethanesulfonic acid (HEPES)/TMAH, pH 7.4, 0.3 M sucrose.
3. Sarco(endo)plasmic reticulum Ca^{2+}-ATPase: The protein source used in the present example is endoplasmic reticulum membranes (microsomes) purified from COS-1 cells transfected with an expression vector containing the gene encoding wild-type or mutant SERCA1a Ca^{2+}-ATPase isoform, according to established procedures [41]. The typical total protein

content of the stock samples is ~10 mg/mL, of which ~1 % is Ca^{2+}-ATPase, corresponding to a typical Ca^{2+}-ATPase concentration of ~1 μM. Dilute in Ca^{2+}-ATPase storage buffer to the desired concentration (*see* **Note 5**).

4. Ca^{2+}-ATPase preincubation buffer: In the present example, the photolabeling is carried out on Ca^{2+}-ATPase stabilized in an *E*2·P phosphate transition state-like conformation by incubation of the Ca^{2+}-deprived enzyme with the phosphate-analog orthovanadate in the following buffer (2×): 50 mM 3-(N-morpholino)propanesulfonic acid (MOPS)/TMAH pH 7.0, 160 mM KCl, 10 mM $MgCl_2$, 4 mM EGTA.
5. 1 mM orthovanadate: 492 μL water/NaOH (pH ~ 10) + 8.17 μL 61.2 mM orthovanadate. The 61.2 mM orthovanadate stock solution is prepared according to established procedures [42].
6. Photolabeling buffer (4×): 100 mM 4-(2-hydroxyethyl)-piperazine-1-propanesulfonic acid (EPPS)/TMAH, pH 8.5, 8 mM EDTA.
7. 0.01–100 μM [γ-^{32}P]TNP-8N_3-ATP dilutions (10× relative to the final reaction mix during photolabeling). The specific activity of the [γ-^{32}P]TNP-8N_3-ATP immediately following its synthesis is much higher than necessary for the photolabeling experiments. Initially, we therefore prepare a 100 μM solution (this typically being the most concentrated solution needed for the photolabeling experiments), in which 1 per 20 mol comes from the newly synthesized radioactive [γ-^{32}P]TNP-8N_3-ATP batch and 19 per 20 mol come from a non-radioactive TNP-8N_3-ATP batch (*see* **Notes 6** and **7**). Less concentrated [γ-^{32}P]TNP-8N_3-ATP solutions (but, importantly, each with the same specific activity) are then prepared by dilution of the 100 μM solution in water. Store the [γ-^{32}P]TNP-8N_3-ATP dilutions on ice during the experiments and at −20 °C otherwise. Over time, as the radioactivity drops (the half-life of the ^{32}P isotope is 14.3 days), we retain a relatively high specific activity in the experiments by preparing new [γ-^{32}P]TNP-8N_3-ATP solutions, in which a larger proportion of the TNP-8N_3-ATP comes from the radioactive batch, until after ~2 months we finally use the radioactive [γ-^{32}P]TNP-8N_3-ATP batch without diluting the radioactivity with nonradioactive TNP-8N_3-ATP. In this manner, we find that each [γ-^{32}P]TNP-8N_3-ATP synthesis can be used reliably for photolabeling experiments for at least 3 months. The azido group is light sensitive, so take care to shield the [γ-^{32}P]TNP-8N_3-ATP solutions from direct light exposure at all times, e.g., by wrapping the tubes containing the [γ-^{32}P]TNP-8N_3-ATP stock dilutions in tinfoil.
8. 87 % glycerol.

9. 10 mM ATP/TMAH, pH 7.5. Filter sterilize and store in small aliquots at –20 °C.
10. Xenon arc light source. We use an LOT-QuantumDesign LSH102 Arc Light Source assembled with a 150 W ozone-free xenon arc lamp, a rear light reflector, an F/1.3 35-mm aperture quartz condenser, and a glass filter with a 295-nm wavelength cut-off (LOT-QuantumDesign, Darmstadt, Germany; *see* **Note 8**).
11. UV safety goggles. Should be worn at all times when operating the xenon arc light source.
12. 300–400 µL quartz cuvette with 1 mm path width and 10 mm path length. We use Hellma Suprasil 300 cuvettes. To permit the insertion of a pipette tip into the cuvette it is important that the cuvette is of the lidded type rather than of the type with a screw cap.
13. 200 µL pipette tips with long and thin (< 1 mm outer diameter) tip ends, to enable the photolabeling mix to be loaded into and extracted from the labeling cuvette.
14. Height-adjustable lab jack. At the center of one of the edges of the lab jack, place a 1×1 cm square piece of colored tape, defining the position of the cuvette during irradiation.
15. Table mini centrifuge (microfuge), for quick spin downs of Eppendorf tubes.
16. Temperature-regulated water bath.

2.3 Sodium Dodecyl Sulfate (SDS)-Polyacrylamide Gel Electrophoresis, Gel Drying, Radiometric Detection, and Data Analysis

1. 10 % (w/v) SDS: Dissolve 50 g SDS in water to a final volume of 500 mL.
2. Resolving gel buffer (4×): 1.5 M Tris–HCl, pH 8.8, 0.4 % SDS. Dissolve 90.8 g Tris in 400 mL water and adjust the pH to 8.8 with HCl. Add 20 mL 10 % SDS and water to a final volume of 500 mL.
3. Stacking gel buffer (4×): 0.5 M Tris–HCl, pH 6.8, 0.4 % SDS. Dissolve 15.2 g Tris in 200 mL water and adjust the pH to 6.8 with HCl. Add 10 mL 10 % SDS and water to a final volume of 250 mL.
4. Gel running buffer (5×): 0.125 M Tris, 0.96 M glycine, 0.5 % SDS. Dissolve 30.3 g Tris and 144.1 g glycine in 1.5 L water. Add 100 mL 10 % SDS and water to a final volume of 2 L.
5. 20 % SDS/bromophenol blue: Dissolve 10 g SDS and a "pinch" of bromophenol blue (*see* **Note 9**) in water to a final volume of 50 mL.
6. β-Mercaptoethanol.
7. Protein denaturation buffer (for 30 samples): Add 90 µL β-mercaptoethanol to 150 µL 20 % SDS/bromophenol blue and vortex. Prepare fresh for each experiment.

8. 30 % acrylamide/bis solution, 37.5:1.
9. *N,N,N′,N′*-Tetramethyl-ethylenediamine (TEMED).
10. 10 % (w/v) ammonium persulfate. Store at 4 °C (*see* **Note 10**).
11. Polyacrylamide gel electrophoresis equipment and power supply: We use the Hoefer SE250 Mighty Small II Mini Vertical Electrophoresis Units with 1.5 mm thickness T-spacers and 1.5 mm thickness 10-well combs (Hoefer Inc., Holliston, MA, USA). Larger gel electrophoresis units may be used instead, such as the Hoefer SE600 Standard Dual Cooled Vertical Unit. The advantage of the larger unit is that more samples and higher sample volumes can be applied compared with the mini gels, at the disadvantage, however, of the electrophoresis being more time consuming (~2 h running time for the mini gels compared with ~4 h for the large gels).
12. Gel drying equipment: We use a Bio-Rad Model 583 Gel Dryer (Bio-Rad) connected via a cold trap to a vacuum pump. It is critical that the vacuum pressure in the gel dryer is < 5 mbar, otherwise the gel bands will get fuzzy.
13. Radiometric detection equipment: *See* **item 33** in Subheading 2.1.
14. Data analysis: We use the SigmaPlot program (Systat Software Inc.) for regression analysis, graphing, and statistical analysis of the quantified gel bands.

3 Methods

Carry out all procedures at room temperature unless otherwise specified. Be aware that the azido group is light sensitive and, thus, care should be taken at all times to shield the $8N_3$-ATP and TNP-$8N_3$-ATP nucleotides from light exposure, in particular from direct sun light (hence, if possible, draw the curtains in the laboratory, at least during the [γ-^{32}P]TNP-$8N_3$-ATP synthesis steps). The polypropylene material of regular laboratory plasticware is generally quite efficient in shielding against the photoactivation of the azido group by regular daylight.

3.1 Preparation of [γ-^{32}P]$8N_3$-ATP: The ^{32}P-Exchange Reaction

The first step in the synthesis of the [γ-^{32}P]TNP-$8N_3$-ATP photolabel is the exchange of the γ-phosphate of $8N_3$-ATP with ^{32}P-labeled phosphate (Fig. 4).

1. Mix the following, in this order, in a 1.5 mL Eppendorf tube (final volume: 0.5 mL): 66 µL water, 50 µL ^{32}P-exchange buffer (10×), 51 µL 100 mM NaOH, 2 µL 500 mM cysteine, 22.5 µL 10 mM $8N_3$-ATP, 5 µL 100 mM d-(−)-3-phosphoglyceric acid, 1.9 µL 27 mg/mL glyceraldehyde 3-phosphate dehydrogenase, 300 µL 10 mCi/mL phosphorus-32 orthophosphoric

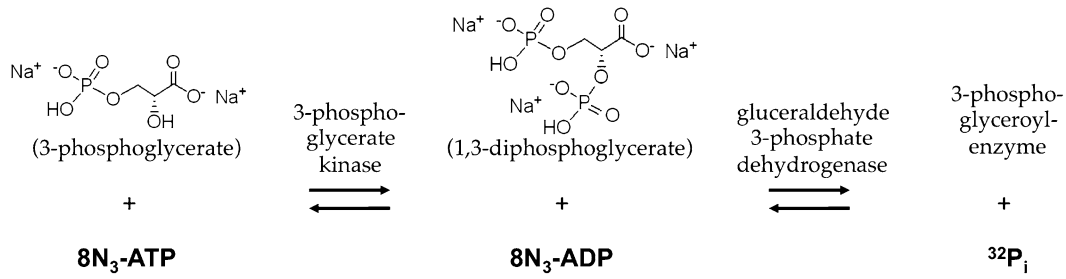

Fig. 4 Principles of the ^{32}P-exchange reaction. The exchange of the γ-phosphate of $8N_3$-ATP with ^{32}P-labeled phosphate is made feasible by the actions of two enzymes, 3-phosphoglycerate kinase and glyceraldehyde 3-phosphate dehydrogenase, in the presence of the suitable substrates [49]. 3-Phosphoglycerate kinase catalyzes the phosphorylation of 3-phosphoglycerate by $8N_3$-ATP, forming 1,3-diphosphoglycerate and $8N_3$-ADP. A complex is then formed between 1,3-diphosphoglycerate and glyceraldehyde 3-phosphate dehydrogenase, leading to the derivatization of this enzyme with phosphoglycerate and concomitant release of phosphate. Because the equilibrium of the former reaction is far towards the left side, and since $8N_3$-ATP is added in excess over phosphate ($^{32}P_i$), over time the vast majority of the ^{32}P-labeled phosphate included in the reaction mix will be incorporated into $8N_3$-ATP, as verified by the results shown in Fig. 5a

acid (~3 mCi). Vortex and collect at the bottom of the tube, and then add 1.25 μL 4 mg/mL 3-phosphoglyceric phosphokinase to initiate the exchange reaction (if the 3-phosphoglyceric phosphokinase supplied by the manufacturer varies in concentration from that used in the present example, adjust the volume accordingly). Vortex, collect at the bottom of the tube, and incubate the tube in a lead container for 2½ h at room temperature with occasional mixing.

2. After 1½ h reaction check for ^{32}P-incorporation by TLC (continue the incubation of the reaction mix at room temperature while the TLC is running): Prepare a TLC sheet strip of 20 cm in length and a couple of centimeters in width. Draw a line lightly with a soft pencil ~2–3 cm from one end of the strip. Spot a minimum amount of the reaction mix (~0.2 μL) on the line. Lower the TLC strip (spotted end first) into a container with ~1 cm of 1 M LiCl (i.e., so that the liquid level does not reach the spot). Place a lid on the container and wait for the solvent to reach ~2 cm from the top of the strip (~30–40 min). Dry the strip with a hair dryer and check for radioactivity by phosphor imaging (Fig. 5a). At this stage, the reaction mix is highly radioactive, so the phosphor screen need only be placed on the TLC strip for ~10–20 s.
3. Prepare a 2 cm (resin height) × 0.5 cm (inner diameter) DE52 anion-exchange column with a 1 mL dead-volume outlet tubing (the column can be prepared while the TLC is running). Rinse the resin by several washings with water prior to its application to the column. Chromatography is carried out by gravity flow. Apply the ^{32}P-exchange reaction mix to the column.

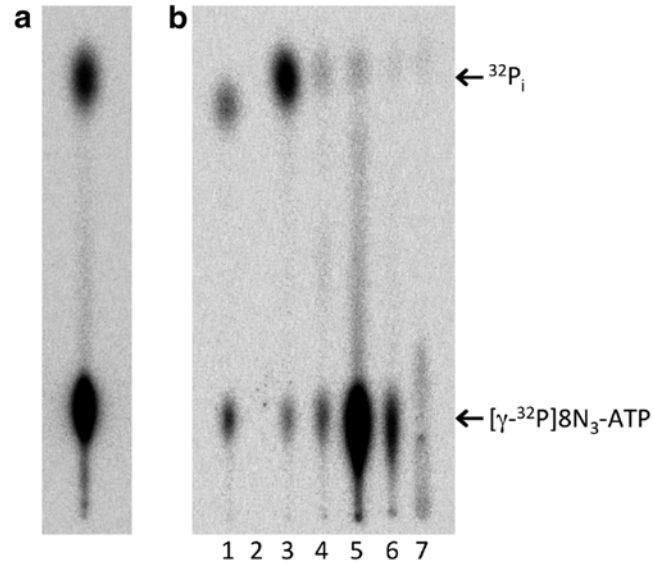

Fig. 5 TLC analysis of the ^{32}P-exchange reaction and purification eluates. (**a**) TLC analysis of the ^{32}P-exchange reaction mix after 1½ h incubation. At this stage, ~90 % of the ^{32}P-labeled phosphate has typically been incorporated into the 8N$_3$-ATP. (**b**) TLC analysis of the eluates from the DE52 anion exchange purification. The eluates correspond to the following additions to the column: *lane 1*, 0.5 mL reaction mix + 0.5 mL water + 5 mL water; *lane 2*, 5 mL 1 mM HCl; *lane 3*, 7 mL 10 mM HCl; *lane 4*, 1 mL 30 mM HCl; *lane 5*, 7 mL 30 mM HCl (main [γ-^{32}P]8N$_3$-ATP fraction); *lane 6*, 2 mL 30 mM HCl; *lane 7*, 5 mL 1 M HCl

Wash the reaction tube with 0.5 mL water and apply to the column. Wash the column with 5 mL water. Acidify the column with 5 mL 1 mM HCl. Elute the phosphate and 8N$_3$-ADP with 7 mL 10 mM HCl. Elute the [γ-^{32}P]8N$_3$-ATP with 30 mM HCl as follows: (a) add 1 mL to the column (dead-volume in tubing), (b) add 7 mL to the column (main [γ-^{32}P]8N$_3$-ATP fraction; collect in a 30 mL freeze-drying flask, wrapped in tinfoil to shield from light), (c) add 2 mL to the column (for control), and (d) add 5 mL 1 M HCl (for control). *See* Fig. 5b for a TLC analysis of the various eluates from the DE52 column.

4. Neutralize the pH of the 7 mL [γ-^{32}P]8N$_3$-ATP fraction with 105 μL 0.8 M Na_2CO_3/$NaHCO_3$, pH 9.5. The pH can be checked by spotting a small volume on a pH indicator strip.
5. Freeze-dry the [γ-^{32}P]8N$_3$-ATP fraction: Freeze the [γ-^{32}P]8N$_3$-ATP solution by lowering the freeze-drying flask into liquid nitrogen for 2–3 min. Place the freeze drying flask on ice in a lidded polystyrene foam thermobox with a small hole in the lid, allowing the vacuum tubing to reach the freeze drying flask. Connect the vacuum to the freeze drying flask and leave overnight.

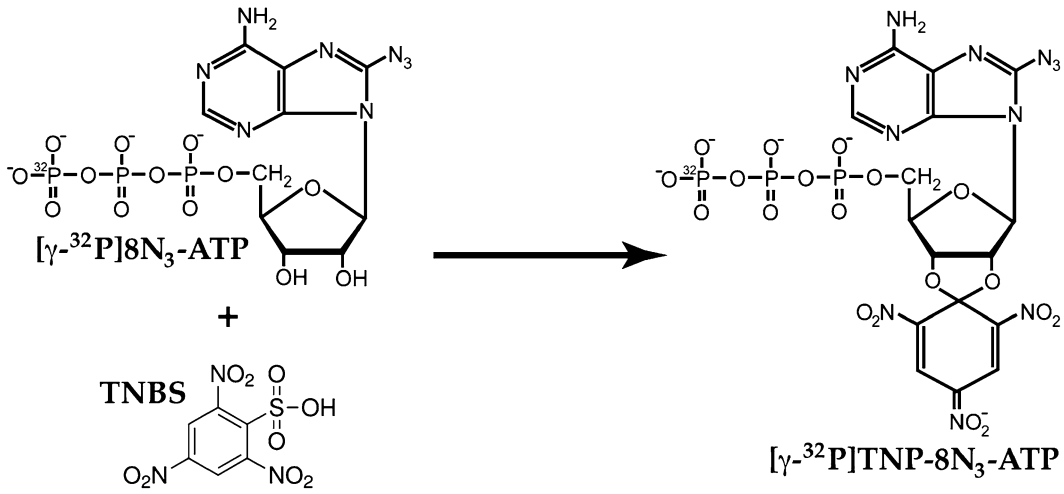

Fig. 6 Principles of the trinitrophenylation reaction. The reaction of the 2′,3′-hydroxyls of the ribose of [γ-^{32}P]8N_3-ATP with TNBS, leading to the formation of [γ-^{32}P]TNP-8N_3-ATP

3.2 Preparation of [γ-^{32}P]TNP-8N_3-ATP: Trinitrophenylation of [γ-^{32}P]8N_3-ATP

The second step in the synthesis of the [γ-^{32}P]TNP-8N_3-ATP photolabel is the addition of the TNP-group to the 2′,3′-hydroxyls of the ribose of [γ-^{32}P]8N_3-ATP (Fig. 6).

1. Check that all the water has evaporated from the freeze drying flask. Add 150 µL water to the flask and dissolve the precipitated [γ-^{32}P]8N_3-ATP by gently moving the water around. Adjust the freeze drying flask to room temperature (>20 °C).
2. Weigh ~13.5 mg DTNB into a 1.5 mL Eppendorf tube (*see* **Note 11**).
3. Thaw a tube of 500 µL 0.8 M Na_2CO_3/$NaHCO_3$, pH 9.5 in a 37 °C water bath. Vortex and repeat the incubation at 37 °C until all the salt crystals have dissolved. Adjust to room temperature.
4. Do the following in rapid succession (NB! at room temperature, not on ice): Transfer the 0.5 mL 0.8 M Na_2CO_3/$NaHCO_3$, pH 9.5 to the tube with DTNB and vortex. Add 40 µL 1 M TNBS to the dissolved DTNB and vortex. Transfer 83 µL of the DTNB/TNBS mix to the freeze-drying flask containing 150 µL [γ-^{32}P]8N_3-ATP and mix by moving the flask around. Incubate at 25 °C (or at room temperature if this is already around 25 ± 3–4 °C) in the dark with occasional mixing.
5. After 2½–3 h reaction check for trinitrophenylation by TLC (following the same procedure described in **step 2** in Subheading 3.1). An example of the typical outcome of this analysis is shown in Fig. 7a.
6. After 4 h reaction add 5 mL ice-cold water to the freeze drying flask. At this point, the reaction mix can be left at −20 °C overnight.

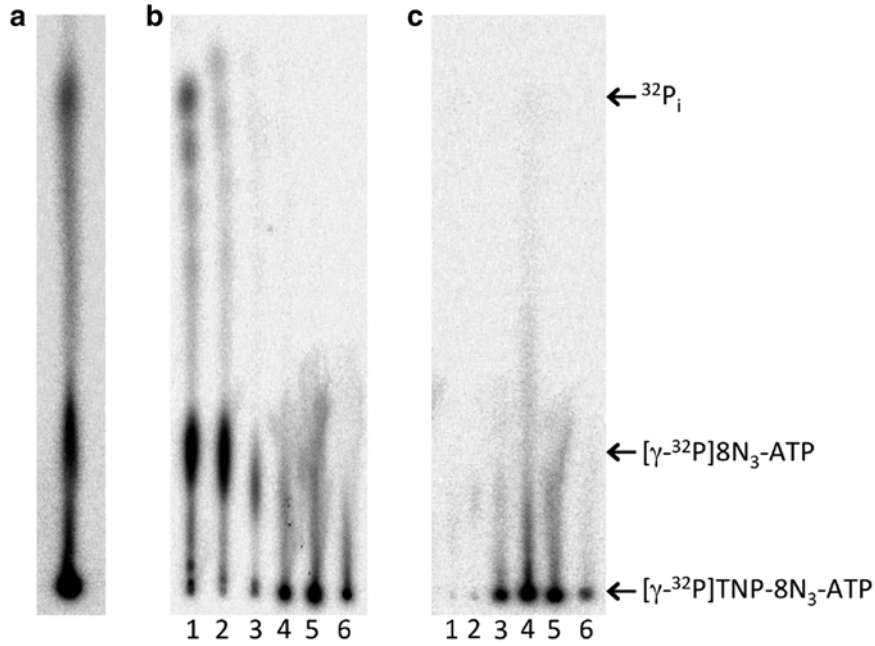

Fig. 7 TLC analysis of the trinitrophenylation reaction and purification eluates. (**a**) TLC analysis of the trinitrophenylation reaction mix after 3 h incubation. (**b**) TLC analysis of the eluates from the DE52 anion-exchange column purification. The eluates correspond to the following additions to the column: *lane 1*, 5.25 mL reaction mix + 6 mL water; *lane 2*, 10 mL 0.2 M ammonium formate pH 8.2; *lane 3*, 15 mL 0.5 M ammonium formate pH 8.2; *lane 4*, 4 mL 1 M ammonium formate pH 8.2; *lane 5*, 21 mL 1 M ammonium formate pH 8.2 (main [γ-^{32}P]TNP-8N_3-ATP fraction); *lane 6*, 5 mL 1 M ammonium formate pH 8.2. (**c**) TLC analysis of the eluates from the Sep-Pak purification. The eluates correspond to the following additions to the Sep-Pak cartridge: *lane 1*, 21 mL main [γ-^{32}P]TNP-8N_3-ATP fraction from the DE52 column; *lane 2*, 2 mL 10 mM KH_2PO_4/K_2HPO_4, pH 7.0; *lane 3*, 0.9 mL water; *lane 4*, 2 mL 60 % acetonitrile (main [γ-^{32}P]8N_3-ATP fraction; a 50-fold dilution of the final product after acetonitrile/water vaporization was spotted); *lane 5*, 2 mL 60 % acetonitrile; *lane 6*, 2 mL 60 % acetonitrile

7. Prepare a 4 cm (resin height) × 0.5 cm (inner diameter) DE52 anion-exchange column with a 2 mL dead-volume outlet tubing (this can be done during the 4 h reaction period). Rinse the resin by several washings with water prior to its application to the column. At this time also prepare the 0.2, 0.5, and 1 M ammonium formate, pH 8.2 solutions.
8. Chromatography is carried out by gravity flow. Apply the reaction mix (~5.25 mL) to the column. Wash the freeze-drying flask with 6 mL water and apply to the column. Elute with ammonium formate as follows: (a) 2× 5 mL 0.2 M ammonium formate, pH 8.2, (b) 3× 5 mL 0.5 M ammonium formate, pH 8.2, (c) 4 mL 1 M ammonium formate, pH 8.2 (dead volume in tubing), (d) 3× 5 mL + 1× 6 mL 1 M ammonium formate, pH 8.2 (main [γ-^{32}P]TNP-8N_3-ATP fraction; collect in a 50 mL plastic tube on ice), and (e) 5 mL 1 M ammonium

formate, pH 8.2 (for control). *See* Fig. 7b for a TLC analysis of the various eluates from the DE52 column. At this point, the 21 mL main [γ-^{32}P]TNP-8N_3-ATP fraction can be left at −20 °C overnight.

9. Prime a Sep-Pak® Plus C18 solid-phase extraction cartridge by applying 6 mL methanol followed by 10 mL water to the cartridge using plastic syringes.
10. Apply the 21 mL main [γ-^{32}P]TNP-8N_3-ATP fraction to the cartridge using a plastic syringe. This is best done as follows: (a) remove the piston from the syringe, (b) connect the syringe to the cartridge, (c) pour the 21 mL main [γ-^{32}P]TNP-8N_3-ATP fraction into the syringe, (d) carefully reinsert the piston into the syringe, and (e) push the piston down and collect the eluate in a suitable container (be aware that the eluate is radioactive).
11. Apply 2 mL 10 mM KH_2PO_4/K_2HPO_4, pH 7.0 to the cartridge using a plastic syringe.
12. Load a 1 mL plastic syringe with 1 mL water and slowly apply water to the cartridge until the [γ-^{32}P]TNP-8N_3-ATP starts eluting. This is easily observable/measurable, as the drops start to turn strongly yellow/orange and start to become highly radioactive. Stop pushing the piston of the syringe immediately after the first highly radioactive yellow/orange drop has been released from the cartridge. This happens after ~0.9 mL of water has been applied.
13. Apply 2 mL 60 % acetonitrile to the cartridge, and collect the eluate (main [γ-^{32}P]TNP-8N_3-ATP fraction) in a 5 mL radioisotope bottle in a lead container.
14. Apply further 2× 2 mL 60 % acetonitrile to the cartridge (for control). *See* Fig. 7c for a TLC analysis of the various eluates from the Sep-Pak purification.
15. Vaporize the acetonitrile, as well as some of the water, from the 2 mL main [γ-^{32}P]TNP-8N_3-ATP fraction by directing a stream of nitrogen gas into the radioisotope bottle through a Pasteur pipette connected via tubing to a nitrogen gas cylinder. Proceed until the final volume is ~300–400 μL, at which point the [γ-^{32}P]TNP-8N_3-ATP concentration will typically be ~200–300 μM, corresponding to a typical molar yield of ~40 % [γ-^{32}P]TNP-8N_3-ATP relative to the amount of 8N_3-ATP (225 nmol) applied at the start of the procedure. The time it takes to reach a volume of 300–400 μL from a starting volume of 2 mL is typically ~1 h.
16. Determine the concentration of [γ-^{32}P]TNP-8N_3-ATP by measuring the light absorbance of the TNP-moiety at 408 and 468 nm in a 100-fold dilution of the [γ-^{32}P]TNP-8N_3-ATP

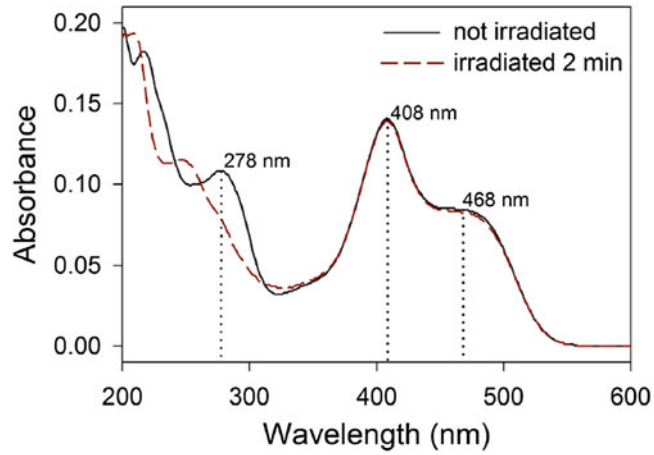

Fig. 8 Absorbance spectrum of [γ-^{32}P]TNP-8N_3-ATP. The absorbance spectrum of the final product of the [γ-^{32}P]TNP-8N_3-ATP synthesis/purification procedure was measured on a 100-fold dilution in 10 mM KH_2PO_4/K_2HPO_4, pH 7.0, before (*solid curve*) and after (*broken curve*) irradiation for 2 min. The peak at 278 nm is attributed to the azido group (which breaks down upon irradiation) and those at 408 and 468 nm to the TNP moiety

solution in 10 mM KH_2PO_4/K_2HPO_4, pH 7.0, using extinction coefficients of 28,000 and 19,300 M^{-1} cm^{-1} for the two wavelengths, respectively (Fig. 8). We define the [γ-^{32}P]TNP-8N_3-ATP concentration as the average of the values measured at 408 and 468 nm.

17. Store the [γ-^{32}P]TNP-8N_3-ATP solution at −20 °C.

3.3 Time Dependence of TNP-8N_3-ATP Photolysis

The rate-limiting step in the photolabeling reaction is the photoactivation of the azido group of TNP-8N_3-ATP, resulting in the formation of the reactive nitrene (Fig. 2; left half of the reaction scheme). The subsequent chemical reaction between the nitrene of the photoactivated nucleotide and Lys^{492} of the Ca^{2+}-ATPase (Fig. 2; right half of the reaction scheme) is likely a much faster reaction, given the typical short life time and high reactivity of nitrene intermediates [12–14]. The irradiation setup we have applied in recent years is shown in Fig. 9. A quartz cuvette containing the labeling reaction mix is placed at a fixed position (e.g., marked by a 1 × 1 cm square piece of colored tape on a lab jack) in front of the light source, with the collimated light beam centered at the part of the cuvette containing the reaction mix. The diameter of the light beam should cover the entire reaction volume contained in the cuvette. Irradiation is then carried out by manually opening the shutter and then closing the shutter again after an appropriate time interval, determined as described in the following. The photoactivation should be performed under pre-steady-state conditions, with an irradiation time interval compatible with

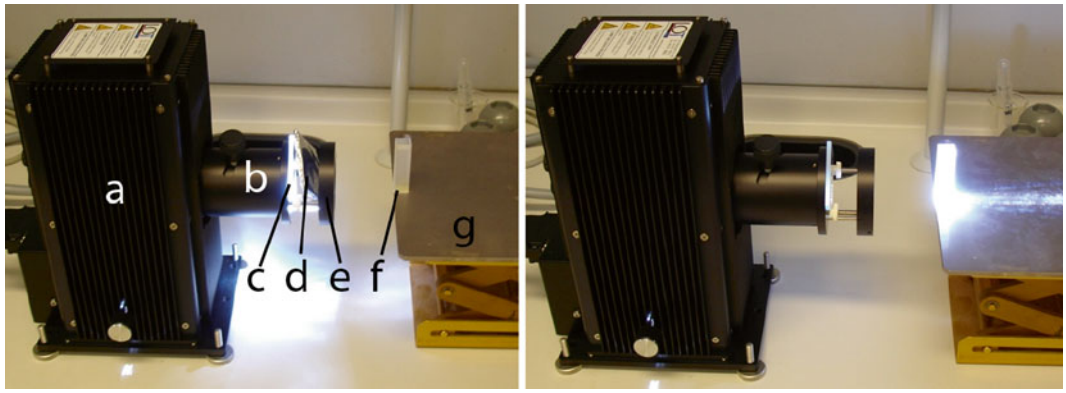

Fig. 9 The irradiation setup. The xenon arc light source irradiation setup with closed (*left panel*) and open (*right panel*) shutter: *a*, lamp housing; *b*, light condenser; *c*, 295-nm wavelength cut-off glass filter; *d*, manually operated light shutter (a square piece of cardboard wrapped in tinfoil); *e*, filter holder; *f*, labeling cuvette; *g*, height-adjustable lab jack

70–80 % photoactivation of the TNP-$8N_3$-ATP photolabel. This time interval is determined by measuring the rate of photoactivation, which can be optimized to individual preferences by adjusting either the intensity of the light source or the distance between the light source and the labeling cuvette. We find that an irradiation time interval of 30–40 s is optimal for the practical handling of the samples during the experiments. With our standard irradiation setup, placing the labeling cuvette at a fixed position 5 cm from the tip of the filter holder mounted in front of the condenser (Fig. 9), setting the power supply of the light source to 38 W, and irradiating the samples for 35 s is compatible with ~75 % photoactivation. This, however, should be optimized (by trial and error) for each individual irradiation setup. The rate of photoactivation of TNP-$8N_3$-ATP is determined as follows:

1. Prepare a 10 μM solution of nonradioactive TNP-$8N_3$-ATP by dilution of the stock solution in 10 mM KH_2PO_4/K_2HPO_4, pH 7.0.
2. Irradiate aliquots of 100 μL of the 10 μM TNP-$8N_3$-ATP solution for varying time intervals.
3. Dilute in 10 mM KH_2PO_4/K_2HPO_4, pH 7.0 to an appropriate volume for spectrophotometrical analysis (e.g., to 400 μL, for absorbance measurements in a 400 μL quartz cuvette) and measure the light absorbance at 278 nm (the absorbance peak of the $8N_3$ group; Fig. 10a).
4. Plot the light absorbance as a function of the irradiation time and extract the rate constant (v) for photoactivation of TNP-$8N_3$-ATP by fitting a monoexponential decay function, $A = A_0 + A\infty \cdot e^{-v \cdot t}$, to the data (Fig. 10b). The time interval giving 75 % labeling is then calculated by the equation $t_{75\,\%} = -(\ln 0.25)/v$.

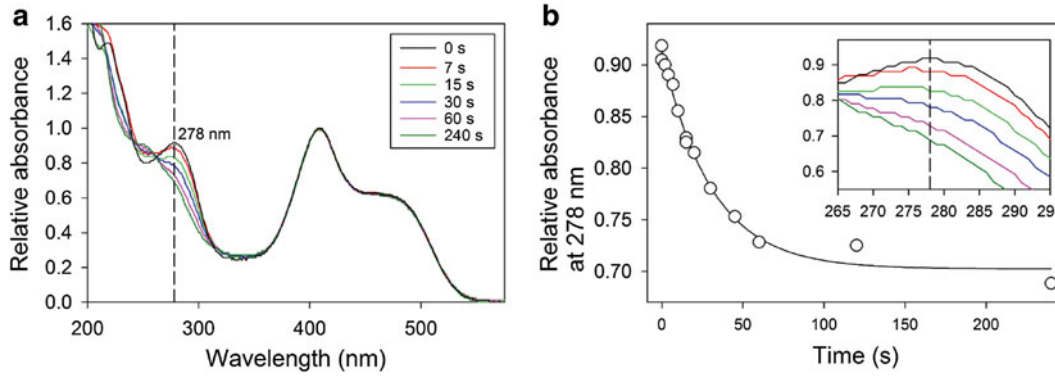

Fig. 10 Time dependence of the photolysis of TNP-8N_3-ATP. (**a**) The absorbance spectrum of TNP-8N_3-ATP was recorded following irradiation for varying time intervals. The absorbance maximum at 278 nm, contributed by the azido group, decreases upon irradiation owing to its degradation (*see* Fig. 2). For comparison, the maximum absorbance at 408 nm (contributed by the TNP-moiety) was set to 1 for all time intervals, and spectra are shown for selected times. (**b**) Graph showing the relative absorbance at 278 nm as a function of the time of irradiation. The *inset* shows a close-up view of the absorbance around 278 nm from panel **a**. These experiments were originally published in The Journal of Biological Chemistry. Clausen JD, McIntosh DB, Woolley DG, and Andersen JP. (2011) Modulatory ATP binding affinity in intermediate states of *E*2P dephosphorylation of sarcoplasmic reticulum Ca^{2+}-ATPase. J Biol Chem 286: 11792–11802. © 2011 by The American Society for Biochemistry and Molecular Biology

3.4 [γ-^{32}P]TNP-8N_3-ATP Dependence of Photolabeling of the Ca^{2+}- ATPase

The ultimate goal of the photolabeling assay is to measure the affinity of the Ca^{2+}-ATPase for ATP, and the first step in the process involves the determination of the $K_{0.5}$ for TNP-8N_3-ATP binding. In the present example, photolabeling is carried out on wild type or mutant F487S Ca^{2+}-ATPase stabilized in an *E*2·P phosphate transition state-like conformation by incubation of Ca^{2+}-deprived enzyme with orthovanadate [16, 43, 44], and the photolabeling buffer contains excess EDTA, to chelate Ca^{2+} and Mg^{2+}, in a pH 8.5 buffer. The assay may, however, be carried out with enzyme stabilized in a multitude of different reaction states and at various buffer conditions (e.g., *see* [10, 16, 19]). Buffers in the pH 8–9 range are generally preferable for photolabeling experiments, owing to reduced labeling levels outside this range and increased levels of unspecific labeling, in particular for the COS-1 expressed enzyme, at pH below 8 [10]. The photolabeling should be carried out one sample at a time. Keep all constituents on ice during the experiment. The following is the protocol for an experiment comprising ten samples with varying concentrations of [γ-^{32}P]TNP-8N_3-ATP (Fig. 11).

1. Stabilization of the enzyme in the *E*2·orthovanadate state: 20 μL Ca^{2+}-ATPase preincubation buffer (2×), 12 μL water, 4 μL 1 mM orthovanadate, 4 μL 250 nM Ca^{2+}-ATPase (to give a final concentration of Ca^{2+}-ATPase in the photolabeling mix of 1 nM). Vortex and incubate for 30 min at 25 °C, followed

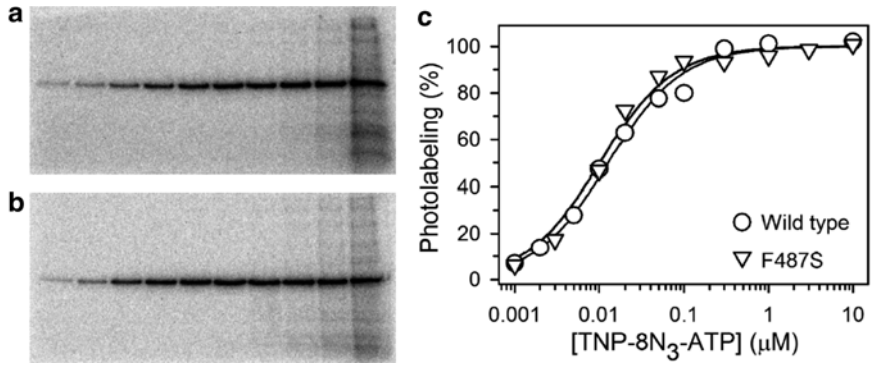

Fig. 11 The [γ-^{32}P]TNP-8N_3-ATP dependence of photolabeling. (**a**, **b**) Autoradiographs of the gels from experiments studying the [γ-^{32}P]TNP-8N_3-ATP dependence of photolabeling on COS-1-expressed wild type (**a**) and mutant F487S (**b**) Ca^{2+}-ATPase stabilized in the *E2*·orthovanadate state. The concentrations of [γ-^{32}P]TNP-8N_3-ATP applied are as indicated on the graph in panel **c**. Note the extraordinary specificity of the labeling reaction. Hence, up to ~1 μM [γ-^{32}P]TNP-8N_3-ATP, i.e., far beyond the $K_{0.5}$ for the photolabel (~10 nM), only one band can be distinguished in the gels, namely that corresponding to the Ca^{2+}-ATPase, regardless of the fact that the Ca^{2+}-ATPase only constitutes ~1 % of the total protein in the sample. At [γ-^{32}P]TNP-8N_3-ATP concentrations above 1 μM other weaker bands start to appear, corresponding to the low-specificity labeling of various other proteins in the sample. (**c**) Analysis of the experiments corresponding to panels **a** and **b** by nonlinear regression. The $K_{0.5}$ (TNP-8N_3-ATP) values extracted from the analysis are wild type, $K_{0.5} = 12.7$ nM; mutant F487S, $K_{0.5} = 10.1$ nM

by at least 10 min on ice (once the *E2*·orthovanadate state is formed, it is stable for hours).

2. Sample premix: 18.75 μL photolabeling buffer (4×), 30.75 μL water. Prepare a batch mix for all samples and aliquot 49.5 μL into 1.5 mL Eppendorf tubes. Incubate on ice.
3. Photolabeling reaction mix: In rapid succession, add 15 μL 87 % glycerol, 7.5 μL [γ-^{32}P]TNP-8N_3-ATP dilution (10×), and 3 μL of the orthovanadate-inhibited 25 nM Ca^{2+}-ATPase to the sample premix (final volume: 75 μL).
4. Vortex, collect at the bottom of the tube, and transfer to the quartz cuvette (pre-cooled on ice). Wipe the labeling side of the cuvette with tissue and place the cuvette on the 1 × 1 cm piece of tape on the lab jack (Fig. 9). Open the shutter of the light source and irradiate the reaction mix for the time interval determined to be compatible with ~75 % photoactivation of photolabel (as determined in the experiments described in Subheading 3.3). Close the shutter of the light source and transfer the reaction mix from the cuvette back to the same Eppendorf tube from which it came. Leave on ice until all samples have been irradiated.
5. Proceed to **step 3** in Subheading 3.6 for gel electrophoretic separation of the samples.

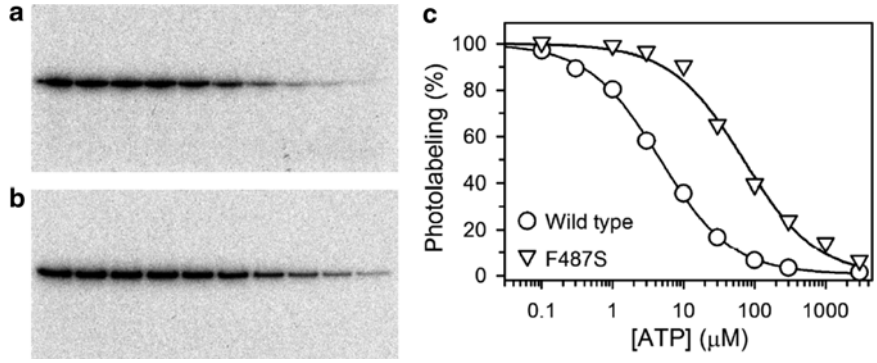

Fig. 12 The ATP dependence of the inhibition of [γ-^{32}P]TNP-8N$_3$-ATP photolabeling. (**a**, **b**) Autoradiographs of the gels from experiments studying the ATP dependence of [γ-^{32}P]TNP-8N$_3$-ATP photolabeling on COS-1-expressed wild type (**a**) and mutant F487S (**b**) Ca^{2+}-ATPase stabilized in the *E2*·orthovanadate state. The concentrations of ATP applied are as indicated on the graph in panel **c** (note that, for both wild type and mutant the first data point on the gel corresponds to 0 μM ATP and is, thus, not visible on the graph owing to the logarithmic scale of the abscissa). (**c**) Analysis of the experiments corresponding to panels **a** and **b** by nonlinear regression. The $K_{0.5}$ (ATP) values and Hill coefficients extracted from the analysis are: wild type, $K_{0.5} = 4.63$ μM, $n = 0.86$; mutant F487S, $K_{0.5} = 69.88$ μM, $n = 0.84$. The experiments were carried out at the standard [γ-^{32}P]TNP-8N$_3$-ATP concentration of 3× $K_{0.5}$ (TNP-8N$_3$-ATP) and, hence, the true dissociation constants for ATP binding are as follows (calculated as described in **step 2** of Subheading 3.7): wild type, $K_D = 1.16$ μM; mutant F487S, $K_D = 17.5$ μM

3.5 Competitive Inhibition by ATP of [γ-^{32}P]TNP-8N$_3$-ATP Photolabeling of the Ca^{2+}- ATPase

In the present example we study the binding of ATP to wild-type and mutant F487S Ca^{2+}-ATPase stabilized in the *E2*·orthovanadate state. The assay is, however, not limited to ATP affinity measurements, but may be applied to measure the affinity of any nucleotide, nucleotide analog, or other substance that competes with TNP-8N$_3$-ATP for binding. The photolabeling is generally carried out at a concentration of [γ-^{32}P]TNP-8N$_3$-ATP in the final reaction mix of 3 × $K_{0.5}$ for TNP-8N$_3$-ATP binding, with the $K_{0.5}$ for TNP-8N$_3$-ATP being as determined in the experiments described in Subheading 3.4. The photolabeling should be carried out one sample at a time. Keep all ingredients on ice during the experiment. The following is the protocol for an experiment comprising ten samples with varying concentrations of ATP (Fig. 12).

1. Stabilize the enzyme in the *E2*·orthovanadate state as described in **step 1** of Subheading 3.4.
2. Sample premix: 18.75 μL photolabeling buffer (4×), 23.25 μL water. Prepare a batch mix for all samples and aliquot 42 μL into 1.5 mL Eppendorf tubes. Incubate on ice.
3. Photolabeling reaction mix: In rapid succession, add 15 μL 87 % glycerol, 7.5 μL ATP dilution (10×), 7.5 μL [γ-^{32}P]TNP-8N$_3$-ATP at a concentration of 30× the $K_{0.5}$ for TNP-8N$_3$-ATP (as determined in the experiments described in Subheading 3.4),

and 3 μL of the orthovanadate-inhibited 25 nM Ca^{2+}-ATPase to the sample premix (final volume: 75 μL).

4. Irradiate the photolabeling reaction mix as described in **step 4** of Subheading 3.4.
5. Proceed to **step 3** in Subheading 3.6 for gel electrophoretic separation of the samples.

3.6 7 % SDS-Polyacrylamide Gel Electrophoresis, Gel Drying, and Phosphor Imaging

In the present example, the gels are prepared using the Hoefer SE250 Mighty Small II Mini Vertical Electrophoresis Units. We typically run four gels per experiment. For convenience, the gels can be prepared 1–2 days in advance (in which case, store the gels in 1× gel running buffer at 4 °C). If other gel running systems are applied, or less/more than four gels are needed, adjust the gel volumes, gel running times, and power supply settings accordingly.

1. Resolving gel: 10 mL resolving gel buffer (4×), 20.4 mL water, 9.33 mL 30 % acrylamide/bis solution, 29 μL TEMED, 234 μL 10 % ammonium persulfate (final volume: 40 mL). Mix gently (do not shake) and pour the gel into the gel caster. Allow space for the stacking gel (the stacking gel need not be very large, 4–5 mm between the tip of the comb and the resolving gel is fine). Overlay with water by pipetting 150 μL of water slowly down along the spacer at both sides of the gel. Wait for the resolving gel to polymerize (15–20 min). Pour the water off the surface of the resolving gel.
2. Stacking gel: 3.75 mL stacking gel buffer (4×), 9.6 mL water, 1.5 mL 30 % acrylamide/bis solution, 9.6 mL water, 12 μL TEMED, 95 μL 10 % ammonium persulfate (final volume: 15 mL). Mix gently (do not shake) and pour the stacking gel on top of the polymerized resolving gel. Insert the 10-well combs. Wait for the stacking gel to polymerize (15–20 min). Top with stacking gel mix (this can be kept on ice to delay polymerization) if the gel level drops during the polymerization.
3. Sample denaturation: Add 8 μL protein denaturation buffer to each 75 μL sample and vortex.
4. Load 35 μL in each lane (*see* **Note 12**) and run the gels in 1× gel running buffer at 15 mA per gel at 4 °C until the bromophenol blue band is ~0.5–1 cm from the bottom of the gel (~2 h).
5. Cut off and discard the bottom ~1.5 cm of the gel. Be aware that this part of the gel is highly radioactive, as it contains the non-reacted [γ-^{32}P]TNP-8N_3-ATP. Hence, be careful not to smear it across the main gel. The Ca^{2+}-ATPase bands will be roughly at the center of the remaining part of the resolving gel.
6. Dry the gel and measure the radioactivity associated with the Ca^{2+}-ATPase gel bands by phosphor imaging.

7. Typical results obtained in experiments measuring the [γ-^{32}P] TNP-8N$_3$-ATP dependence of photolabeling and the ATP-dependence of the inhibition of photolabeling are shown in Figs. 11 and 12, respectively, exemplified by experiments with COS-1-expressed wild-type and mutant F487S Ca^{2+}-ATPase.

3.7 Data Analysis

The photolabeling data is analyzed by nonlinear regression, applying the previously validated equations [10].

1. The analysis of the TNP-8N$_3$-ATP dependence of photolabeling (Fig. 11) is based on the hyperbolic function $\Upsilon = \Upsilon_{max} \cdot [\text{TNP-8N}_3\text{-ATP}]/(K_{0.5} + [\text{TNP-8N}_3\text{-ATP}])$, in which Υ is the amount of photolabeled Ca^{2+}-ATPase, Υ_{max} is the maximum amount of photolabeled Ca^{2+}-ATPase, and $K_{0.5}$ is the concentration of TNP-8N$_3$-ATP giving half-maximum labeling. In some cases, typically when working with poorly expressed protein or in situations where the affinity for TNP-8N$_3$-ATP is particularly low, it may be necessary to include a linear component to account for secondary/unspecific labeling occasionally observed at high TNP-8N$_3$-ATP concentrations: $\Upsilon = \Upsilon_{max} \cdot [\text{TNP-8N}_3\text{-ATP}]/(K_{0.5} + [\text{TNP-8N}_3\text{-ATP}]) + m \cdot [\text{TNP-8N}_3\text{-ATP}]$, where m is the slope of the linear component.
2. The analysis of the data obtained from the ATP inhibition of TNP-8N$_3$-ATP photolabeling (Fig. 12) is based on the Hill equation modified to describe inhibition, $\Upsilon = \Upsilon_{max} \cdot (1 - [\text{ATP}]n)/(K_{0.5}n + [\text{ATP}]n)$, in which Υ and Υ_{max} are defined as above, $K_{0.5}$ is the concentration of ATP giving half-maximum inhibition of labeling, and n is the Hill coefficient (typically displaying a value of around 0.7–1.0, in accordance with the presence of one binding site for ATP). The "true" dissociation constant, K_D, for ATP binding is calculated from the equation K_D (ATP) = $K_{0.5}$ (ATP)/(1 + [TNP-8N$_3$-ATP]/$K_{0.5}$ (TNP-8N$_3$-ATP)), where [TNP-8N$_3$-ATP] is the concentration of TNP-8N$_3$-ATP applied in the ATP titration experiment. Given that the ATP dependence of photolabeling is generally performed at a concentration of TNP-8N$_3$-ATP of 3 × $K_{0.5}$ (TNP-8N$_3$-ATP), the equation simply becomes K_D (ATP) = $K_{0.5}$ (ATP)/(1 + 3/1) = $K_{0.5}$ (ATP)/4 (*see* **Note 13**).

4 Notes

1. As an alternative to using the commercially available 8N$_3$-ATP, this nucleotide can be synthesized from ATP by bromination of the adenine moiety at the 8-position, followed by replacement of the bromine with an azido group, according to established procedures [11, 45].

2. It is critical that the ^{32}P-labeled orthophosphate used is carrier-free, i.e., not supplemented with nonradioactive phosphate. We use product number NEX053H (10 mCi/mL) from PerkinElmer.
3. The procedure requires the handling of a rather large amount (~3 mCi = 111 Mbq) of ^{32}P, a beta particle-emitting radioactive isotope. Hence, it is essential to take the necessary precautions, such as frequently monitoring the workspace with a Geiger-Müller counter and shielding the radioactive material behind thick acrylic glass protection and/or in thick-walled lead containers at all times. Diligently follow all waste disposal regulations when disposing the radioactive materials.
4. It is critical that TMAH is used instead of Tris for the pH adjustment of all reaction buffers applied in the photolabeling experiments, because the presence of Tris will lead to increased background labeling levels, owing to the reaction of the amino group of Tris with the azido group of [γ-^{32}P]TNP-8N_3-ATP upon UV irradiation. Be aware that TMAH is toxic.
5. It is advisable to have a good and reliable estimate of the Ca^{2+}-ATPase concentration of the protein sample applied, to ensure that the [γ-^{32}P]TNP-8N_3-ATP is in excess of the Ca^{2+}-ATPase during photolabeling. It is critical that the Ca^{2+}-ATPase concentration is kept well below the $K_{0.5}$ for [γ-^{32}P]TNP-8N_3-ATP, which under some reaction conditions may get as low as 5–10 nM. Hence, it is sometimes necessary to keep the Ca^{2+}-ATPase concentration in the final photolabeling reaction mix as low as 0.5–1 nM.
6. The nonradioactive TNP-8N_3-ATP is prepared in the same way as the radioactive [γ-^{32}P]TNP-8N_3-ATP, except that the ^{32}P-exchange reaction step is skipped, and that the reaction is scaled up by applying 6.7-fold more 8N_3-ATP as starting material, i.e., starting from **step 2** in Subheading 3.2 with 150 μL 10 mM 8N_3-ATP (in this case, the reaction need not be done in the freeze drying flask, but can simply be carried out in a 1.5 mL Eppendorf tube).
7. Example of the preparation of a 100 μM [γ-^{32}P]TNP-8N_3-ATP working solution for photolabeling experiments: Assuming we have a 200 μM radioactive [γ-^{32}P]TNP-8N_3-ATP batch and a 1 mM non-radioactive TNP-8N_3-ATP batch, and that we want to prepare 200 μL of a 100 μM [γ-^{32}P]TNP-8N_3-ATP solution with the specific activity being diluted 20-fold relative to the newly synthesized [γ-^{32}P]TNP-8N_3-ATP batch. 200 μL × 100 μM = 20 nmol total TNP-8N_3-ATP, of which 1 nmol must come from the radioactive batch and 19 nmol must come from the non-radioactive batch (corresponding to a 20-fold dilution of the radioactivity). Hence, to 176 μL of

water add 5 μL 200 μM [γ-^{32}P]TNP-8N_3-ATP (=1 nmol) and 19 μL 1 mM TNP-8N_3-ATP (=19 nmol).

8. It is important that the UV light is filtered, because short wavelength UV light is harmful to the protein (*see* Supplementary Fig. S3 in [16]). As an alternative to the 295-nm wavelength cut-off glass filter one can also filter the UV light by placing a quartz cuvette, with a 10 mm path length and a > 1 mm path width, containing toluene in front of the labeling cuvette (toluene has a rather steep light absorbance cut-off around 270–275 nm).
9. The exact amount of bromophenol blue is not very important. A few mg, e.g., corresponding to the amount that will stick to a (sterile) plastic pipette tip when dipped into the jar of bromophenol blue, is typically fine. The purpose of the bromophenol blue is just to give color to the electrophoretic front during gel running, thus indicating visibly how far the gel has run. Since the bromophenol blue gets stacked during the run, even small amounts of bromophenol blue are easily visible in the gels.
10. It is commonly stated that the 10 % ammonium persulfate used for the preparation of polyacrylamide gels must be prepared fresh. We, however, find that the solution, when stored at 4 °C, can easily be used for a month without any noticeable decrease in the quality of the gels.
11. The amount of DTNB does not need to be very precise, as anywhere between 12 and 15 mg DTNB will give the same result. The oxidizing agent DTNB prevents the reduction of the azido group by sulfonic acid and also increases the yield of the trinitriphenylation reaction. Other oxidizing agents, such as H_2O_2, are also applicable; however DTNB was found to give the best yield [11].
12. The final sample volume after adding the protein denaturation buffer is 83 μL. With the Hoefer SE250 Mighty Small II Mini Vertical Electrophoresis Units with 1.5 mm spacers/combs it is possible to load a maximum of ~45 μL per lane. We generally load 35 μL per lane, but run two gels per 10-sample experiment (thus loading each sample on two separate gels). In our experience, the step in the procedure, where problems are most likely to occur, is the gel running (individual samples that for one reason or another run atypically on the gel). By running two gels for each experiment we minimize the risk of an effect on the final result by any samples "lost" on the gels.
13. In cases where the affinity for TNP-8N_3-ATP is particularly low, it can be an advantage to carry out the experiments at a lower concentration of [γ-^{32}P]TNP-8N_3-ATP, e.g., at 1 × $K_{0.5}$ (TNP-8N_3-ATP) instead of at 3 × $K_{0.5}$ (TNP-8N_3-ATP), to prevent background labeling levels from affecting the result.

Be aware, though, that if a concentration of [γ-^{32}P]TNP-8N_3-ATP other than 3 × $K_{0.5}$ (TNP-8N_3-ATP) is applied, this should be taken into account when calculating the K_D (ATP). For example, if a concentration of 1 × $K_{0.5}$ (TNP-8N_3-ATP) is applied, the K_D (ATP) is given by $K_{0.5}$ (ATP)/(1 + 1/1) = $K_{0.5}$ (ATP)/2.

Acknowledgements

This work was supported by the Lundbeck Foundation and the Centre for Membrane Pumps in Cells and Disease—PUMPKIN, Danish National Research Foundation (to JDC), the National Research Foundation, South Africa, and the University of Cape Town, South Africa (to DBM and DGW), and the Danish Medical Research Council and the Novo Nordisk Foundation (to JPA).

References

1. Lacapere JJ, Bennett N, Dupont Y, Guillain F (1990) pH and magnesium dependence of ATP binding to sarcoplasmic reticulum ATPase. Evidence that the catalytic ATP-binding site consists of two domains. J Biol Chem 265(1):348–353
2. Lacapere JJ, Guillain F (1993) The reaction mechanism of Ca(2+)-ATPase of sarcoplasmic reticulum. Direct measurement of the Mg.ATP dissociation constant gives similar values in the presence or absence of calcium. Eur J Biochem 211(1-2):117–126
3. Norby JG, Jensen J (1971) Binding of ATP to brain microsomal ATPase. Determination of the ATP-binding capacity and the dissociation constant of the enzyme-ATP complex as a function of K^+ concentration. Biochim Biophys Acta 233(1):104–116
4. Hegyvary C, Post RL (1971) Binding of adenosine triphosphate to sodium and potassium ion-stimulated adenosine triphosphatase. J Biol Chem 246(17):5234–5240
5. Fedosova NU, Champeil P, Esmann M (2003) Rapid filtration analysis of nucleotide binding to Na,K-ATPase. Biochemistry 42(12): 3536–3543
6. Vilsen B, Andersen JP, MacLennan DH (1991) Functional consequences of alterations to amino acids located in the hinge domain of the Ca(2+)-ATPase of sarcoplasmic reticulum. J Biol Chem 266(24):16157–16164
7. Sorensen T, Vilsen B, Andersen JP (1997) Mutation Lys758 → Ile of the sarcoplasmic reticulum Ca^{2+}-ATPase enhances dephosphorylation of E2P and inhibits the E2 to E1Ca2 transition. J Biol Chem 272(48): 30244–30253
8. Sorensen TL, Dupont Y, Vilsen B, Andersen JP (2000) Fast kinetic analysis of conformational changes in mutants of the Ca(2+)-ATPase of sarcoplasmic reticulum. J Biol Chem 275(8): 5400–5408
9. Vilsen B (1993) Glutamate 329 located in the fourth transmembrane segment of the alpha-subunit of the rat kidney Na^+,K^+-ATPase is not an essential residue for active transport of sodium and potassium ions. Biochemistry 32(48):13340–13349
10. McIntosh DB, Woolley DG, Vilsen B, Andersen JP (1996) Mutagenesis of segment 487Phe-Ser-Arg-Asp-Arg-Lys492 of sarcoplasmic reticulum Ca^{2+}-ATPase produces pumps defective in ATP binding. J Biol Chem 271(42): 25778–25789
11. Seebregts CJ, McIntosh DB (1989) 2′,3′-O-(2,4,6-Trinitrophenyl)-8-azido-adenosine mono-, di-, and triphosphates as photoaffinity probes of the Ca^{2+}-ATPase of sarcoplasmic reticulum. Regulatory/superfluorescent nucleotides label the catalytic site with high efficiency. J Biol Chem 264(4): 2043–2052
12. Chowdhry V, Westheimer FH (1979) Photoaffinity labeling of biological systems. Annu Rev Biochem 48:293–325
13. Kotzyba-Hibert F, Kapfer I, Goeldner M (1995) Recent trends in photoaffinity labeling. Angew Chem Int Ed Engl 34:1296–1312

14. Potter RL, Haley BE (1983) Photoaffinity labeling of nucleotide binding sites with 8-azidopurine analogs: techniques and applications. Methods Enzymol 91:613–633
15. Suzuki H, Kubota T, Kubo K, Kanazawa T (1990) Existence of a low-affinity ATP-binding site in the unphosphorylated Ca2(+)-ATPase of sarcoplasmic reticulum vesicles: evidence from binding of 2′,3′-O-(2,4,6-trinitrocyclohexadienylidene)-[3H]AMP and -[3H]ATP. Biochemistry 29(30): 7040–7045
16. Clausen JD, McIntosh DB, Woolley DG, Andersen JP (2011) Modulatory ATP binding affinity in intermediate states of E2P dephosphorylation of sarcoplasmic reticulum Ca^{2+}-ATPase. J Biol Chem 286(13):11792–11802
17. McIntosh DB, Woolley DG, Berman MC (1992) 2′,3′-O-(2,4,6-Trinitrophenyl)-8-azido-AMP and -ATP photolabel Lys-492 at the active site of sarcoplasmic reticulum Ca(2+)-ATPase. J Biol Chem 267(8): 5301–5309
18. McIntosh DB, Woolley DG (1994) Catalysis of an ATP analogue untethered and tethered to lysine 492 of sarcoplasmic reticulum Ca(2+)-ATPase. J Biol Chem 269(34):21587–21595
19. McIntosh DB, Woolley DG, MacLennan DH, Vilsen B, Andersen JP (1999) Interaction of nucleotides with Asp(351) and the conserved phosphorylation loop of sarcoplasmic reticulum Ca(2+)-ATPase. J Biol Chem 274(36): 25227–25236
20. Clausen JD, McIntosh DB, Woolley DG, Andersen JP (2001) Importance of Thr-353 of the conserved phosphorylation loop of the sarcoplasmic reticulum Ca^{2+}-ATPase in MgATP binding and catalytic activity. J Biol Chem 276(38):35741–35750
21. Clausen JD, McIntosh DB, Vilsen B, Woolley DG, Andersen JP (2003) Importance of conserved N-domain residues Thr441, Glu442, Lys515, Arg560, and Leu562 of sarcoplasmic reticulum Ca^{2+}-ATPase for MgATP binding and subsequent catalytic steps. Plasticity of the nucleotide-binding site. J Biol Chem 278(22):20245–20258
22. McIntosh DB, Clausen JD, Woolley DG, MacLennan DH, Vilsen B, Andersen JP (2003) ATP binding residues of sarcoplasmic reticulum Ca(2+)-ATPase. Ann N Y Acad Sci 986:101–105
23. McIntosh DB, Clausen JD, Woolley DG, MacLennan DH, Vilsen B, Andersen JP (2004) Roles of conserved P domain residues and Mg^{2+} in ATP binding in the ground and Ca^{2+}-activated states of sarcoplasmic reticulum Ca^{2+}-ATPase. J Biol Chem 279(31):32515–32523
24. Clausen JD, McIntosh DB, Woolley DG, Anthonisen AN, Vilsen B, Andersen JP (2006) Asparagine 706 and glutamate 183 at the catalytic site of sarcoplasmic reticulum Ca^{2+}-ATPase play critical but distinct roles in E2 states. J Biol Chem 281(14):9471–9481
25. Clausen JD, McIntosh DB, Anthonisen AN, Woolley DG, Vilsen B, Andersen JP (2007) ATP-binding modes and functionally important interdomain bonds of sarcoplasmic reticulum Ca^{2+}-ATPase revealed by mutation of glycine 438, glutamate 439, and arginine 678. J Biol Chem 282(28):20686–20697
26. Clausen JD, McIntosh DB, Woolley DG, Andersen JP (2008) Critical interaction of actuator domain residues arginine 174, isoleucine 188, and lysine 205 with modulatory nucleotide in sarcoplasmic reticulum Ca^{2+}-ATPase. J Biol Chem 283(51):35703–35714
27. Clausen JD, Bublitz M, Arnou B, Montigny C, Jaxel C, Moller JV, Nissen P, Andersen JP, le Maire M (2013) SERCA mutant E309Q binds two Ca(2+) ions but adopts a catalytically incompetent conformation. EMBO J 32(24): 3231–3243
28. Clausen JD, Anthonisen AN, Andersen JP (2014) Critical role of interdomain interactions for modulatory ATP binding to sarcoplasmic reticulum Ca^{2+}-ATPase. J Biol Chem 289(42): 29123–29134
29. Sorensen TL, Moller JV, Nissen P (2004) Phosphoryl transfer and calcium ion occlusion in the calcium pump. Science 304(5677): 1672–1675
30. Toyoshima C, Mizutani T (2004) Crystal structure of the calcium pump with a bound ATP analogue. Nature 430(6999):529–535
31. Jensen AM, Sorensen TL, Olesen C, Moller JV, Nissen P (2006) Modulatory and catalytic modes of ATP binding by the calcium pump. EMBO J 25(11):2305–2314
32. Olesen C, Picard M, Winther AM, Gyrup C, Morth JP, Oxvig C, Moller JV, Nissen P (2007) The structural basis of calcium transport by the calcium pump. Nature 450(7172):1036–1042
33. Moczydlowski EG, Fortes PA (1981) Characterization of 2′,3′-O-(2,4,6-trinitrocyclohexadienylidine)adenosine 5′-triphosphate as a fluorescent probe of the ATP site of sodium and potassium transport adenosine triphosphatase. Determination of nucleotide binding stoichiometry and ion-induced changes in affinity for ATP. J Biol Chem 256(5):2346–2356
34. Moczydlowski EG, Fortes PA (1981) Inhibition of sodium and potassium adenosine triphosphatase by 2′,3′-O-(2,4,6-trinitrocyclo-

hexadienylidene) adenine nucleotides. Implications for the structure and mechanism of the Na:K pump. J Biol Chem 256(5):2357–2366

35. Faller LD (1989) Competitive binding of ATP and the fluorescent substrate analogue 2′,3′-O-(2,4,6-trinitrophenylcyclohexadienylidine) adenosine 5′-triphosphate to the gastric H^+, K^+-ATPase: evidence for two classes of nucleotide sites. Biochemistry 28(16): 6771–6778
36. Faller LD (1990) Binding of the fluorescent substrate analogue 2′,3′-O-(2,4,6-trinitrophenylcyclohexadienylidene)adenosine 5′-triphosphate to the gastric H^+,K^+-ATPase: evidence for cofactor-induced conformational changes in the enzyme. Biochemistry 29(13):3179–3186
37. Axelsen KB (2014) The P-type ATPase Database. http://traplabs.dk/patbase/. Accessed 24 Aug 2014
38. Axelsen KB, Palmgren MG (1998) Evolution of substrate specificities in the P-type ATPase superfamily. J Mol Evol 46(1):84–101
39. Decottignies A, Grant AM, Nichols JW, de Wet H, McIntosh DB, Goffeau A (1998) ATPase and multidrug transport activities of the overexpressed yeast ABC protein Yor1p. J Biol Chem 273(20):12612–12622
40. de Wet H, McIntosh DB, Conseil G, Baubichon-Cortay H, Krell T, Jault JM, Daskiewicz JB, Barron D, Di Pietro A (2001) Sequence requirements of the ATP-binding site within the C-terminal nucleotide-binding domain of mouse P-glycoprotein: structure-activity relationships for flavonoid binding. Biochemistry 40(34):10382–10391
41. Maruyama K, MacLennan DH (1988) Mutation of aspartic acid-351, lysine-352, and lysine-515 alters the Ca^{2+} transport activity of the Ca^{2+}-ATPase expressed in COS-1 cells. Proc Natl Acad Sci U S A 85(10):3314–3318
42. Ko YH, Bianchet M, Amzel LM, Pedersen PL (1997) Novel insights into the chemical mechanism of ATP synthase. Evidence that in the transition state the gamma-phosphate of ATP is near the conserved alanine within the P-loop of the beta-subunit. J Biol Chem 272(30): 18875–18881
43. Pick U (1982) The interaction of vanadate ions with the Ca-ATPase from sarcoplasmic reticulum. J Biol Chem 257(11):6111–6119
44. Dupont Y, Bennett N (1982) Vanadate inhibition of the Ca^{2+}-dependent conformational change of the sarcoplasmic reticulum Ca^{2+}-ATPase. FEBS Lett 139(2):237–240
45. Owens JR, Haley BE (1984) Synthesis and utilization of 8-azidoguanosine 3′-phosphate 5′-[5′-32P]phosphate. Photoaffinity studies on cytosolic proteins of Escherichia coli. J Biol Chem 259(23):14843–14848
46. Gourdon P, Liu XY, Skjorringe T, Morth JP, Moller LB, Pedersen BP, Nissen P (2011) Crystal structure of a copper-transporting PIB-type ATPase. Nature 475(7354):59–64
47. Toyoshima C, Yonekura S, Tsueda J, Iwasawa S (2011) Trinitrophenyl derivatives bind differently from parent adenine nucleotides to Ca^{2+}-ATPase in the absence of Ca^{2+}. Proc Natl Acad Sci U S A 108(5):1833–1838
48. Sarma RH, Lee CH, Evans FE, Yathindra N, Sundaralingam M (1974) Probing the interrelation between the glycosyl torsion, sugar pucker, and the backbone conformation in C(8) substituted adenine nucleotides by 1H and 1H-(31P) fast Fourier transform nuclear magnetic resonance methods and conformational energy calculations. J Am Chem Soc 96(23):7337–7348
49. Glynn IM, Chappell JB (1964) A simple method for the preparation of 32-P-labelled adenosine triphosphate of high specific activity. Biochem J 90(1):147–149